

# A high velocity ionised outflow and soft X-ray photosphere in the narrow emission line quasar PG1211+143

K.A.Pounds,<sup>1</sup> J.N.Reeves,<sup>1,2</sup> A.R.King,<sup>1</sup> K.L.Page,<sup>1</sup> P.T.O'Brien,<sup>1</sup> and M.J.L.Turner,<sup>1</sup>

<sup>1</sup> Department of Physics and Astronomy, University of Leicester, Leicester, LE1 7RH, UK

<sup>2</sup> Laboratory for High Energy Astrophysics, NASA Goddard Space Flight Center, Greenbelt, MD 20771, USA

arXiv:astro-ph/0303603v1 27 Mar 2003

Accepted ; Submitted

## ABSTRACT

We report on the analysis of a  $\sim 60$  ksec *XMM-Newton* observation of the bright, narrow emission line quasar PG1211+143. Absorption lines are seen in both EPIC and RGS spectra corresponding to H- and He-like ions of Fe, S, Mg, Ne, O, N and C. The observed line energies indicate an ionised outflow velocity of 0.08–0.1c. The highest energy lines require a column density of  $N_H \sim 5 \times 10^{23} \text{ cm}^{-2}$ , at an ionisation parameter of  $\log \xi \sim 3.4$ . If the origin of this high velocity outflow lies in matter being driven from the inner disc, then the flow is likely to be optically thick within a radius  $\sim 100 R_s$ , providing a natural explanation for the strong soft X-ray excess (and Big Blue Bump) in PG1211+143.

**Key words:** galaxies: active – galaxies: Seyfert: general – galaxies: individual: MKN 766 – X-ray: galaxies

## 1 INTRODUCTION

One of the most striking recent developments in X-ray studies of AGN has been the observation, from high resolution grating spectra with *Chandra* and *XMM-Newton*, of complex absorption indicating circumnuclear (often outflowing) matter existing in a wide range of ionisation states (eg Sako et al. 2001, Kaspi et al. 2002). To date, however, it has generally been assumed that this so-called ‘warm absorber’ was essentially transparent in the ‘Fe K spectral band’ above  $\sim 6$  keV, with fluorescent line emission from the accretion disc being the main feature in AGN spectra at those energies (eg Reynolds and Nowak 2002).

In this paper we report on the spectral analysis of a  $\sim 60$  ksec *XMM-Newton* observation of the bright quasar PG1211+143. At a redshift  $z = 0.0809$  (Marziani et al. 1996) PG1211+143 has a typical X-ray luminosity (2–10 keV) of  $\sim 10^{44}$  erg s $^{-1}$ , for  $H_0 = 75 \text{ km s}^{-1} \text{ Mpc}^{-1}$ . The Galactic absorption column towards PG1211+143 is  $N_H = 2.85 \times 10^{20} \text{ cm}^{-2}$  (Murphy et al. 1996), rendering it visible over the whole ( $\sim 0.2$ –12 keV) spectral band of the EPIC and RGS instruments on *XMM-Newton*.

PG1211+143 is a low redshift, optically bright quasar, with a strong ‘Big Blue Bump’ (BBB). However, it is unusual in the PG sample of bright quasars in having relatively narrow permitted optical emission lines (Boroson and Green 1992, Kaspi 2000). PG1211+143 was first detected in the X-ray band by *Einstein*, which found an unusually

steep spectrum in the  $\sim 0.2$ –2 keV band (Bechtold et al. 1997, Elvis et al. 1991). A subsequent analysis by Saxton et al. (1993), which combined *EXOSAT* and *GINGA* data, resolved a strong soft X-ray ‘excess’ above a harder power component of photon index  $\Gamma \sim 2.1$ . An early *ASCA* observation showed the soft excess to be variable, indicating a source region of  $\leq 10^{15} \text{ cm}$  (Yaqoob et al. 1994). The improved spectral resolution of *ASCA* further refined the broad-band X-ray description of PG1211+143 (Reeves et al. 1997), with evidence for a broad Fe K emission line (equivalent width  $\text{EW} \sim 400$ –750 eV) at  $\sim 6.4$  keV. A more recent study of the overall (infra-red to X-ray) spectrum of PG1211+143 has been published by Janiuk et al. (2001), considering in particular the strong emission in the UV and soft X-ray bands and proposing its origin in a warm optically thick ‘skin’ on the accretion disc. This work also included an analysis of an extended *RXTE* observation in 1997, suggesting a cold reflection factor  $R = \Omega/2\pi$ , where  $\Omega$  is the solid angle subtended by the reflecting matter, of  $\sim 1$ .

## 2 OBSERVATION AND DATA REDUCTION

PG1211+143 was observed by *XMM-Newton* on 2001 June 15 yielding a useful exposure of  $\sim 60$  ksec. In this paper we use data from the EPIC pn camera (Strüder et al. 2001), which has the best sensitivity of any instrument flown to date in the  $\sim 6$ –10 keV spectral band, the combined EPIC

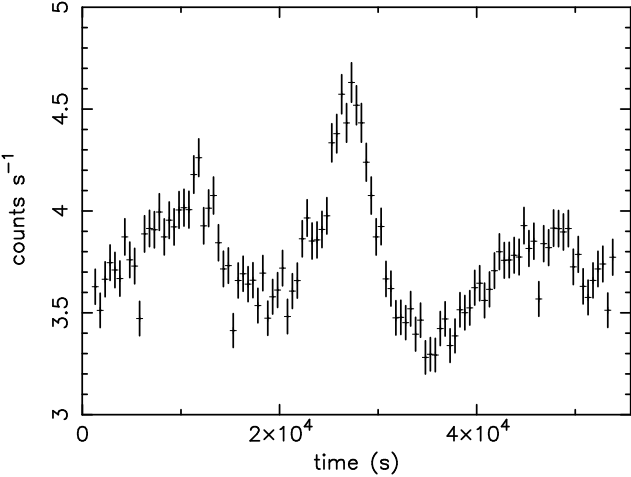


**Figure 1.** X-ray light curve at 0.2–10 keV from the *XMM-Newton* pn observation of PG1211+143 on 2001 June 15.

MOS cameras (Turner et al. 2001), and the Reflection Grating Spectrometer/RGS (den Herder et al. 2001). Reference to the Optical Monitor confirmed the strong optical and UV emission was close to the typical level in PG1211+143. All X-ray data were first screened with the XMM SAS v5.3 software and events corresponding to patterns 0–4 (single and double pixel events) were selected for the pn data and patterns 0–12 for MOS1 and MOS2, the latter then being combined. A low energy cut of 200 eV was applied to all X-ray data and known hot or bad pixels were removed. We extracted source counts within a circular region of 45'' radius defined around the centroid position of PG1211+143, with the background being taken from a similar region, offset from but close to the source. The 0.2–10 keV X-ray pn light curve is reproduced as figure 1 and shows ∼30 percent flux changes over ∼6 ksec, similar to those seen in the *ASCA* data. Individual spectra were binned to a minimum of 20 counts per bin, to facilitate use of the  $\chi^2$  minimisation technique in spectral fitting. Response functions for spectral fitting to the RGS data were generated from the SAS v5.3.

Spectral fitting was based on the Xspec package (Arnaud 1996) and used a grid of ionised absorber models calculated with the XSTAR code (Kallman et al. 1996). All spectral fits include absorption due to the line-of-sight Galactic column of  $N_H = 2.85 \times 10^{20} \text{ cm}^{-2}$ . Errors are quoted at the 90% confidence level ( $\Delta\chi^2 = 2.7$  for one interesting parameter).

### 3 1–10 KEV SPECTRUM

#### 3.1 Power law

X-ray spectra of AGN at 2–10 keV are well fitted, to first order, with a power law of photon index  $\Gamma$  in the range ∼1.6–2 for most radio quiet AGN, with a fraction (eg NLS1) having somewhat steeper indices. The widely held view is that this ‘hard’ X-ray continuum in Seyfert galaxies arises by Comptonisation of thermal emission from the accretion disc in a ‘hot’ corona (eg Haardt and Maraschi 1991), and produces

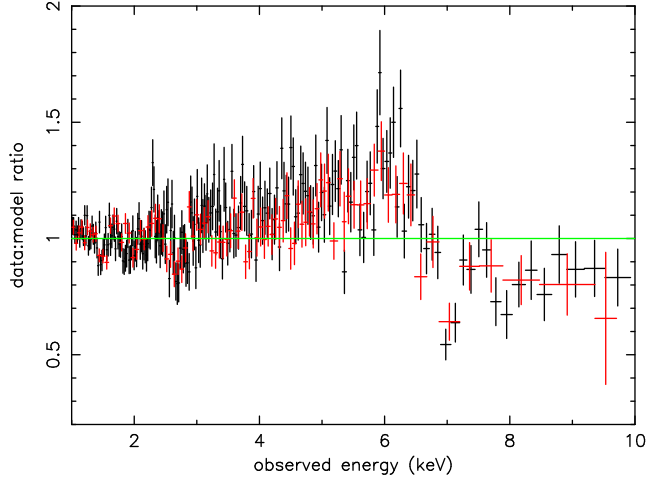


**Figure 2.** Ratio of the EPIC pn (black) and MOS (red) spectral data to a simple power law model fitted between 1–10 keV for PG1211+143. The plot shows a broad excess at 3–7 keV and several absorption features including a deep narrow absorption line near 7 keV.

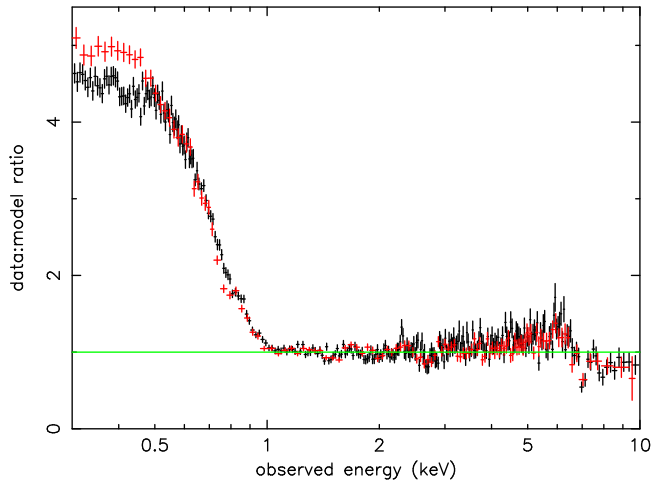


**Figure 3.** Extension to 0.3 keV of the 1–10 keV power law model fits for the pn (black) and MOS (red) spectral data, showing the strong soft excess in PG1211+143.

additional spectral features by ‘reflection’ from dense matter in the disc (eg Pounds et al. 1990, Fabian et al. 2000).

We began our analysis of PG1211+143 by confirming there were no obvious spectral changes with source flux and then proceeded to fit the *XMM-Newton* pn and MOS data integrated over the full ∼60 ksec observation. A simple power law fit over the 1–10 keV band yielded a photon index of  $\Gamma \sim 1.79$  (pn) and  $\Gamma \sim 1.71$  (MOS), with a broad excess in the data:model ratio between 3–7 keV, and evidence of absorption at higher energies in both data sets (figure 2). The fit was statistically unacceptable with an overall  $\chi^2/\text{dof}$  of 1541/1176. When extrapolated to 0.3 keV, the 1–10 keV fits to both pn and MOS data revealed a strong ‘soft excess’ (figure 3).

### 3.2 Fe K emission and absorption features

To improve the 1–10 keV fit we added further spectral components to match the most obvious features in the data. The indication of an extreme broad emission line suggested reflection from the inner accretion disc, conventionally modelled with a LAOR line in Xspec (Laor 1991). The addition of a LAOR line, with inclination initially fixed at 30° and  $R_{out}=100R_g$  (where  $R_g = GM/c^2$  is the gravitational radius for mass  $M$ ), resulted in a significant statistical improvement ( $\chi^2/\text{dof}$  of 1304/1172), but with an unrealistically large EW of  $\sim 1.4$  keV (pn) and  $\sim 1.1$  keV (MOS). To better fit the broad line profile we added a gaussian line with energy tied to that of the LAOR line. (Physically such a gaussian line could represent emission from larger radii on the disc). This addition gave a further improvement in the fit, to  $\chi^2/\text{dof}$  of 1278/1167. The LAOR line still had a high EW  $\sim 0.6$ –0.9 keV, with disk emissivity index  $\beta \sim 3.5$ , and inner disc radius  $R_{in} \sim 1.5R_g$ . The gaussian emission line component had an rms width  $\sigma = 0.28 \pm 0.15$  keV and EW =  $0.25 \pm 0.11$  keV. The (poorly constrained) joint line energy was  $\sim 6.2$  keV, or  $\sim 6.7$  keV in the source rest frame, implying reflection from highly ionised matter.

We then attempted to fit the narrow absorption features visible in figure 2, initially with gaussian shaped absorption lines in Xspec. Adding a gaussian line with energy, width and equivalent width free gave a significantly better fit to the absorption near 7 keV than an absorption edge. The observed line energy was  $7.02 \pm 0.03$  keV, with an rms width of  $50 \pm 50$  eV, and an EW of  $95 \pm 20$  eV. The addition of this gaussian absorption line improved the fit to  $\chi^2/\text{dof} = 1246/1164$ . A second gaussian line at  $7.92 \pm 0.04$  keV was less significant, reducing  $\chi^2$  to 1238 for 1161 dof. In this case a statistically better fit was obtained with an absorption edge at  $\sim 7.7$  keV ( $\chi^2/\text{dof}$  of 1228/1165), which might be due to a blend of absorption lines (of Fe K-beta, or K-alpha of NiXXVII), absorption edges of less highly ionised Fe (XVII or higher), or inner shell transitions as recently addressed by Palmeri et al. (2002). A higher (outflow) velocity component of the absorption line seen at  $\sim 7$  keV is a further possibility. Figure 2 suggests the presence of other narrow absorption features in the EPIC data, the most significant at  $\sim 2.7$  keV, and near 1.5 keV. Fitting these 2 features by successively adding gaussians lines to the model yielded reductions in  $\chi^2$  of, respectively, 26 and 32 for 3 fewer dof in each case. Details of all 3 absorption lines thus identified in the EPIC data are summarised in Table 1. When corrected for the redshift of PG1211+143, each line energy indicates an origin in the same relativistic outflow, with a velocity of  $\sim 27000$ – $30000$  km s $^{-1}$ . The best determined line profile, for the line at  $\sim 7.02$  keV, is essentially unresolved, corresponding to a velocity dispersion of  $\leq 12000$  km s $^{-1}$ . We shall see in Section 3.5 that a tighter line width constraint is obtained from the RGS data.

In summary, we find the 1–10 keV spectrum of PG1211+143 can be described by an extreme relativistic Fe K emission line, together with absorption features which are best fitted with gaussian line profiles rather than absorption edges. The proposed identification of these lines, with resonance absorption from H-like ions of Fe, S, and Mg, indicates an origin in outflowing ionised gas at a velocity  $\sim 0.09$ – $0.1c$ .

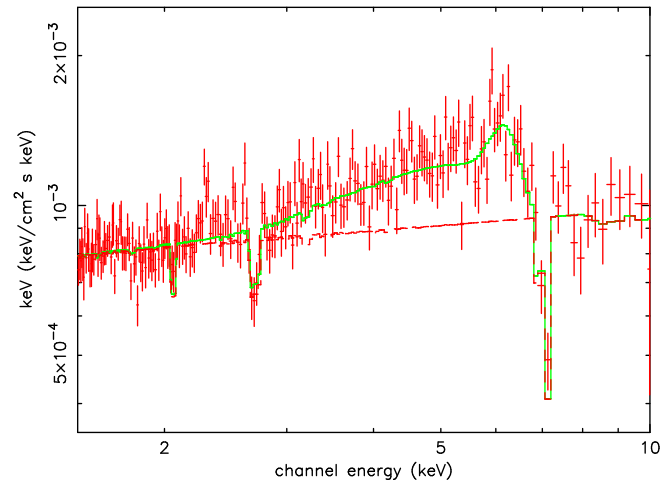


**Figure 4.** Unfolded spectrum illustrating the XSTAR fit to the *XMM-Newton* observation of PG1211+143 as detailed in Section 3.3. For clarity we only show the pn data.

### 3.3 An ionised absorber model

To quantify the highly ionised matter responsible for the observed absorption features we then replaced the gaussian absorption lines in the above model with a grid of photoionised absorbers based on the XSTAR code. These model absorbers cover a wide range of column density and ionisation parameter, with outflow (or inflow) velocities as a variable parameter. All abundant elements from C to Fe are included with the relative abundances as a variable input parameter. In order to limit processing time the fits assume a fixed width of each absorption line of 1000 km s $^{-1}$  FWHM. An absorber with ionisation parameter of  $\log \xi = L/nr^2 \sim 3.4$ , and column density of  $N_H = 5 \times 10^{23} \text{ cm}^{-2}$ , for solar abundances, was found to reproduce the observed absorption line strengths near 7 keV and 2.7 keV (figure 4), assuming their proposed identification with the Lyman alpha lines of FeXXVI and SXVI, and an outflow velocity of  $\sim 0.1c$ . We note that most of the uncertainty in the derived column density is on the upside, since partial covering and accounting for saturation in the relatively narrow line profiles would both increase the above value. The feature attributed to MgXII, and the absorption observed near  $\sim 8$  keV were not modelled by the  $\log \xi = L/nr^2 \sim 3.4$  absorber, indicating the presence of additional absorbing matter at a lower level of ionisation (or a higher velocity outflow component). The implication of a relativistic outflow at a lower ionisation suggests that corresponding features should be evident in the *XMM-Newton* RGS spectrum. We examine that prediction in Section 3.5.

### 3.4 Soft Excess

Extending the 1–10 keV power law fits for both pn and MOS spectral data to 0.3 keV shows very clearly (figure 3) the strong soft excess first indicated by *Einstein* and *EXOSAT* observations (Elvis et al. 1991, Saxton et al. 1993). In the EPIC data this can be adequately modelled with the addition of black body emission components together with 2 surrogate absorption edges. The parameters for PG1211+143 are a primary blackbody of  $kT \sim 110$  eV with a weaker component of  $kT \sim 265$  eV, and ‘edges’ at energies of  $\sim 0.8$  and

**Table 1.** Absorption lines identified in the parametric fit to the combined EPIC spectrum of PG1211+143. Line energies and each ion threshold energy are in keV.

Line	$E_{obs}$	$E_{source}$	$E_{lab}$	velocity (km s $^{-1}$ )	EW (eV)	Ionisation	$\chi^2$
FeXXVI L-alpha	7.02 $\pm$ 0.03	7.59	6.96	27200 $\pm$ 1300	95 $\pm$ 20	8.83	32
SXVI L-alpha	2.69 $\pm$ 0.03	2.90	2.62	32000 $\pm$ 3400	32 $\pm$ 9	3.22	26
MgXII L-alpha	1.49 $\pm$ 0.02	1.61	1.47	28600 $\pm$ 4100	15 $\pm$ 6	1.76	32

$\sim$ 0.98 keV. We note that a similar combination of black body emission superimposed by absorption edges has been found previously to be a good parameterisation of EPIC spectra of AGN (eg. Pounds et al. 2003), though - interestingly - in the present case the edge energies are some 10 percent higher than if associated with the OVII and OVIII edges (at rest). Based on this fit we obtain an average 0.3–10 keV flux for PG1211+143 of  $7.5 \times 10^{-12}$  erg s $^{-1}$  cm $^{-2}$ , corresponding to a luminosity of  $\sim 10^{44}$  erg s $^{-1}$  ( $H_0 = 75$  km s $^{-1}$  Mpc $^{-1}$ ). The blackbody component is dominant in the 0.3–1 keV band, representing  $\sim$ 75 percent of the total flux in that band. The 2–10 keV flux was  $2.7 \times 10^{-12}$  erg s $^{-1}$  cm $^{-2}$ , with a corresponding luminosity of  $3.3 \times 10^{43}$  erg s $^{-1}$ .

### 3.5 Absorption lines in the RGS spectrum

The strongest absorption lines in the EPIC spectrum have been identified with Lyman alpha of FeXXVI and SXVI. The ionisation energy necessary to produce these ions is respectively 8.83 keV and 3.22 keV, which determines the high ionisation parameter in the relevant XSTAR fit. The detection of additional absorption in the EPIC data, including an absorption line attributed to MgXII at 1.47 keV, suggests the ionised outflow includes matter over a range of ionisation states, and should be evident in the RGS spectra of PG1211+143. To check this, we began by jointly fitting the RGS-1 and RGS-2 data with a power law and black body continuum (from the EPIC fit) and examining the residuals by eye. The most obvious spectral features were found to be in absorption, as is often the case with Seyfert 1 spectra, a broad line tentatively identified with the forbidden line of OVII (observed at  $\sim$ 23.75 Angstrom) being the most obvious emission line. A number of weak absorption features are seen which are probably due to Fe L shell absorption, but we concentrate here on the relatively unambiguous identifications associated with H- and He-like resonance absorption in C, N, O and Ne, since these offer a direct confirmation of the ionised outflow seen in the EPIC spectrum. Figures 5–8 show the combined RGS1 and RGS2 spectra with the best fit XSTAR model superimposed. We retained the high ionisation absorber fitted to the EPIC data in the XSTAR mode, and added an intermediate ionisation component to better reproduce the observed absorption in C, N, O and Ne. A third, low ionisation component was added to match the Fe L edge near 17 Angstrom. The best-fit parameters of this model were:

(1)  $N_H = 4 \times 10^{23}$  cm $^{-2}$  at an ionisation parameter of  $\log \xi \sim 3.4$ ;

(2)  $N_H = 6 \times 10^{21}$  cm $^{-2}$  at an ionisation parameter of  $\log \xi \sim 1.7$ ;

(3)  $N_H = 8 \times 10^{22}$  cm $^{-2}$  at an ionisation parameter of  $\log \xi \sim 0.9$ .

Importantly, a large outflow velocity was confirmed from this fit with both of the highly ionised components yielding a velocity of  $\sim 24000$  km s $^{-1}$ .

A visual examination of the RGS spectrum was then carried out to determine the individual line energies, check the line identifications, and hence the deduced outflow velocities. Although quite deep, the individual line profiles are not very well determined due to the limited statistics in the PG1211+143 data, and this is reflected in the estimated uncertainty on the outflow velocities. Nevertheless, we conclude there is no doubt on the identification of the listed lines and their consistent ‘blueshift’. The results of this visual check, summarised in Table 2, yield a weighted mean outflow velocity for the H-like ions of C, N, O and Ne of 23800 km s $^{-1}$ . As noted above, the individual line profiles are not well determined, but are clearly narrow. Since the line width relates directly to the deduced column densities, we produced a ‘combined’ Lyman alpha profile from the RGS data, which is shown in figure 9. This plot confirms the lines to be remarkably narrow, with a measured FWHM of 2000 km s $^{-1}$ , or  $\leq$ 1000 km s $^{-1}$  after allowing for the RGS resolution. Comparison with the measured outflow velocity suggests the material is streaming outward with relatively little turbulence, and that we are viewing down (rather than across) the flow. Importantly, the narrow line widths suggest the high column densities inferred from the XSTAR fits may be underestimates, when allowance is made for possible saturation in the narrow line core. Infill by re-emission (which should be correspondingly small) and our assumption in the model fit of a 100 percent covering factor, both underline the derived column density being a lower limit. The only obvious emission feature in the RGS spectrum, observed at  $\sim$ 23.8 Å ( $\lambda_{lab} = 22.1$  Å), is most likely due to OVII forbidden line emission dispersed across the outflow. Unlike the absorption lines, this line is resolved in the RGS data, with FWHM  $\sim$ 6000 km s $^{-1}$ . The measured EW is  $165 \pm 30$  mA, a part of which may be due to OVII resonance and intercombination line emission.

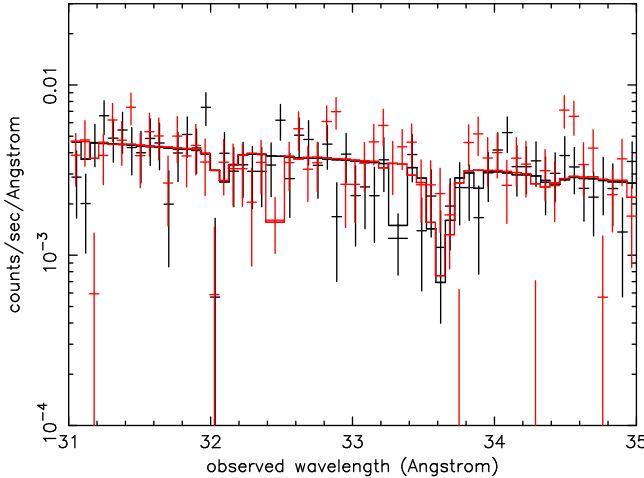
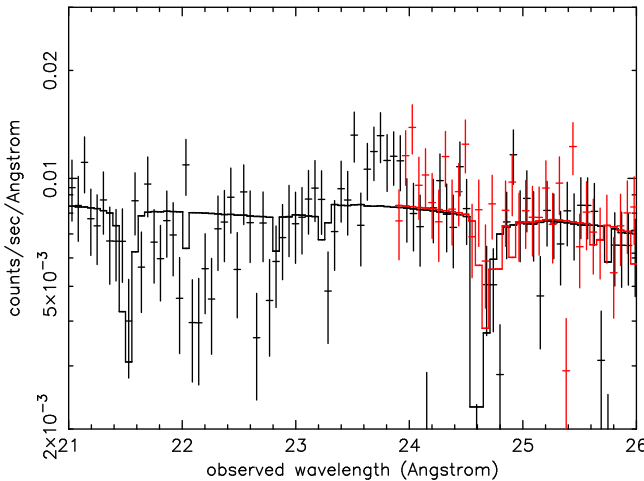
## 4 DISCUSSION

Analysis of the *XMM-Newton* observation of PG1211+143 has revealed several remarkable features.

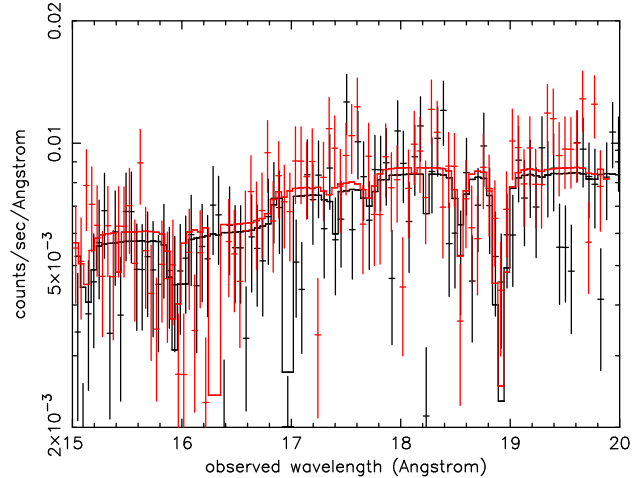
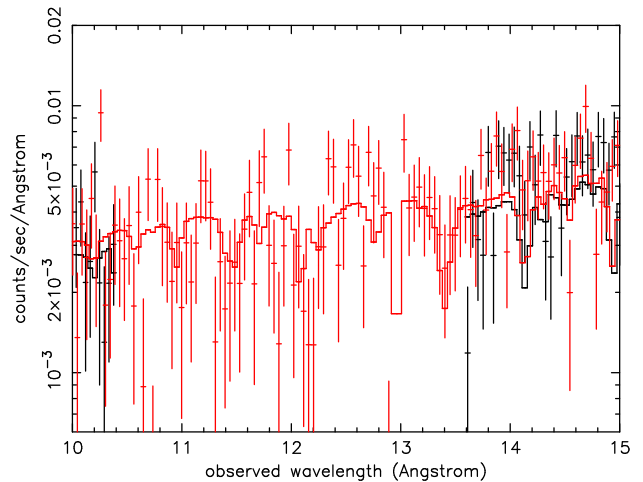
The unusually strong soft excess indicated in previous observations is confirmed. The dominance of this component below  $\sim 1$  keV suggests an origin as intrinsic thermal emission from the accretion disc, though it has long been known that the temperature of a standard ‘thin disc’ is too low in AGN to radiate strongly in the X-ray band. Comptonisation of cooler disc photons in a warm ‘skin’ on the disc surface

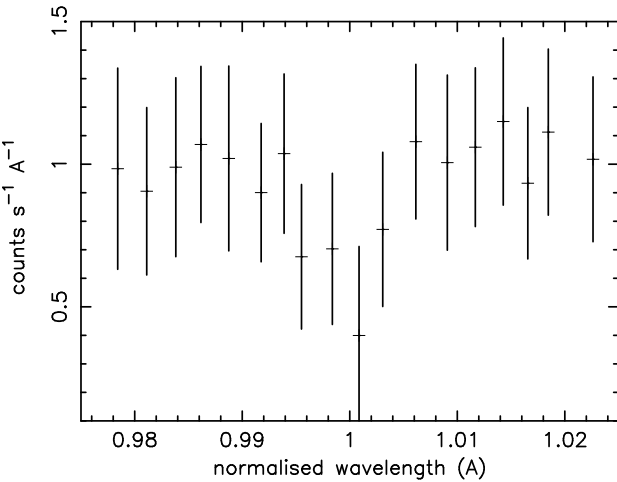
**Table 2.** Absorption lines identified in the RGS spectrum of PG1211+143. All wavelengths in Angstroms

Line	$\lambda_{obs}$	$\lambda_{source}$	$\lambda_{lab}$	velocity km s <sup>-1</sup>	EW (mA)	Ionisation (keV)
NeX L-alpha	12.07 $\pm$ 0.03	11.17	12.13	23700 $\pm$ 800	50 $\pm$ 20	1.20
NeIX 1s-2p	13.40 $\pm$ 0.05	12.40	13.45	23400 $\pm$ 1100	70 $\pm$ 15	0.239
OVIII L-beta	15.98 $\pm$ 0.07	14.78	16.01	23000 $\pm$ 1300	60 $\pm$ 25	0.739
OVIII L-alpha	18.90 $\pm$ 0.03	17.49	18.97	23400 $\pm$ 470	120 $\pm$ 25	0.739
OVII 1s-2p	21.55 $\pm$ 0.05	19.94	21.60	23100 $\pm$ 700	60 $\pm$ 15	0.138
OVII 1s-3p	18.60 $\pm$ 0.05	17.21	18.63	22900 $\pm$ 810	25 $\pm$ 10	0.138
NVII L-alpha	24.78 $\pm$ 0.03	22.93	24.78	22400 $\pm$ 360	50 $\pm$ 10	0.552
CVI L-alpha	33.62 $\pm$ 0.03	31.10	33.72	23300 $\pm$ 270	90 $\pm$ 25	0.392


**Figure 5.** RGS spectrum from 31–35 Angstrom fitted with the photoionised model described in Section 3.5. The CVI Lyman-alpha absorption line is observed at 33.62 Angstrom.

**Figure 6.** RGS spectrum from 21–26 Angstrom showing resonance absorption lines at 21.55 Angstrom (OVII 1s-2p) and 24.78 Angstrom (NVII Lyman-alpha). A broad emission feature at  $\sim$ 23.8 Angstrom is identified with the OVII forbidden line.

has previously been invoked as an explanation of the soft X-ray excess in PG1211+143 (eg Janiuk et al. 2001), while Bechtold et al. (1987) first suggested the soft X-ray flux was a physical extension of the BBB bump, which is particularly strong in PG1211+143 and contains much of the bolomet-


**Figure 7.** RGS spectrum from 15–20 Angstrom showing resonance absorption lines at 18.90 Angstrom (OVII Lyman-alpha), 18.60 Angstrom (OVII 1s-3p) and 15.98 Angstrom (OVIII Lyman-beta)

**Figure 8.** RGS spectrum from 10–15 Angstrom showing absorption lines at 13.40 Angstrom (NeIX 1s-2p) and 12.17 Angstrom (NeX Lyman alpha). Several Fe L lines are also seen and we note that both Ne lines are probably blended with lines of Fe XVII–XXI, limiting their present value in characterising the outflow from PG1211+143



**Figure 9.** A composite profile of the Lyman alpha lines of CV, NV11, OVIII and NeX showing the relatively narrow line width discussed in Section 3.5.

ric luminosity. We suggest an alternative explanation of this dominant ‘thermal emission’ in Section 4.2.

A second notable feature in the EPIC spectrum is the broad Fe K line emission, exhibiting an extreme ‘red wing’. We note that the extreme parameters of this emission line, including the equivalent width, are reduced (but not removed) when absorption visible in the 7–10 keV band is accounted for. We suggest a possible alternative to the ‘relativistic’ Fe K emission line in Section 4.3.

The most interesting revelation in the *XMM-Newton* observation of PG1211+143 is the discovery of an absorption line structure, in both EPIC and RGS data, indicating a high column, high ionisation absorber outflowing at velocities of up to 0.1c. There is marginal evidence of the outflow velocities being higher for the higher energy ions, in the opposite sense to that expected for a simple radiation-driven wind, though this conclusion rests entirely on the (less well determined) EPIC line energies.

#### 4.1 A high velocity ionised outflow.

Previous high resolution X-ray spectra of Seyfert 1 galaxies have found evidence for a broad range of (low to moderate) ionisation states and outflow velocities of typically 100–1000 km s<sup>−1</sup>. The long *Chandra* exposure of the Seyfert galaxy NGC 3783 is a template of such studies (Kaspi et al. 2002). However, until now, any absorption in the Fe K band (above  $\sim 7$  keV) has generally been attributed to continuum (edge) absorption associated with reflection from the accretion disc. A recent exception was the report of an absorption feature in the X-ray spectrum of a high redshift BAL quasar (APM 08279+5255), which has been alternatively identified with the absorption edge of Fe XV–XVIII (Hasinger et al. 2002), or with strongly blue-shifted resonance absorption lines of Fe XXV or XXVI (Chartas et al. 2002). An earlier *ASCA* observation also found evidence for an ‘absorption line’ superimposed on the ‘red wing’ of a broad Fe K emission line in the Seyfert galaxy NGC 3516 (Nandra et al. 1999). The question remains whether highly ionised gas capable of imparting Fe K absorption features on AGN spectra is a significant component in the outflow of most AGN, and is simply

remaining undetected due to the poor sensitivity of current observations of AGN spectra above  $\sim 7$  keV. In the latter respect it may be instructive to note that ionised resonance absorption lines of Fe XXV and XXVI have been seen in the *Chandra* HETGS spectrum of the (much brighter) microquasar GRS 1915+105 (Lee et al. 2002).

An important aspect of our present observations is that the column density of ionised matter in the line-of-sight is high. In the case of PG1211+143 we find an equivalent hydrogen column (assuming solar abundances) approaching  $10^{24}$  cm<sup>−2</sup>. Although the geometry of the outflow (and density) are unknown, it is a reasonable expectation that near its source the flow is optically thick. The interesting consequence, which we explore in Section 4.2, is that the outflow predicts an inner ‘photosphere’ which is then a natural source of the soft X-ray emission (and of a major part of the BBB).

Other important implications following from the detection of a high column, high velocity outflow in PG1211+143 are a high mass loss and a kinetic energy comparable to the observed bolometric luminosity. By comparing the ionisation parameter and column density from the EPIC line fits, with an ionising hard X-ray luminosity of  $5 \times 10^{43}$  erg s<sup>−1</sup>, we estimate a particle density of  $4 \times 10^8$  cm<sup>−3</sup> at a radial distance of  $1.5 \times 10^{15}$  cm. Assuming a spherically symmetric flow into a cone of semi-angle 30° (implying PG1211+143 will turn out to be not be a particularly rare quasar), at an outflow velocity of 0.1c, the mass loss rate is then of order  $0.12 M_{\odot}$  yr<sup>−1</sup>. Assuming the measured outflow velocity is the same as the launch velocity (ie the material is ‘coasting’) then the associated kinetic energy is  $2 \times 10^{43}$  erg s<sup>−1</sup>.

#### 4.2 A soft X-ray photosphere

The previous subsection shows that the column density of the outflow seen in PG1211+143 is close to being optically thick in the continuum. In fact this is inevitable if the mass outflow rate is comparable to the accretion rate required to power radiation at the Eddington limit, as the following calculation shows.

We assume that the outflow quickly reaches a terminal velocity  $v$  and thereafter coasts. Then mass conservation shows that the outflow density is

$$\rho = \frac{\dot{M}}{4\pi v b r^2} \quad (1)$$

at radius  $r$ , where  $\dot{M}$  is the mass loss rate and  $b \leq 1$  allows for collimation of the outflow. The electron scattering optical depth through the outflow, viewed from infinity down to radius  $R$ , is

$$\tau = \int_R^{\infty} \kappa \rho dr = \frac{\kappa \dot{M}}{4\pi v b R} \quad (2)$$

where  $\kappa \simeq \sigma_T / m_H$  is the opacity. The Eddington accretion rate is

$$\dot{M}_{\text{Edd}} = \frac{4\pi GM}{\eta c^2} \quad (3)$$

where  $\eta c^2$  is the accretion yield from unit mass. Combining these equations then gives

$$\tau = \frac{1}{2\eta b} \frac{R_s}{R} \frac{c}{v} \frac{\dot{M}}{\dot{M}_{\text{Edd}}} \quad (4)$$

where  $R_s = 2GM/c^2$  is the Schwarzschild radius for mass  $M$ . Defining the photospheric radius  $R_{\text{ph}}$  as the point  $\tau = 1$  gives

$$\frac{R_{\text{ph}}}{R_s} = \frac{1}{2\eta b} \frac{c}{v} \frac{\dot{M}}{\dot{M}_{\text{Edd}}} \simeq \frac{5}{b} \frac{c}{v} \frac{\dot{M}}{\dot{M}_{\text{Edd}}} \quad (5)$$

where we have taken  $\eta \simeq 0.1$  at the last step. Since  $b \leq 1, v/c < 1$  we see that  $R_{\text{ph}} > R_s$  for any outflow rate  $\dot{M}$  of order  $\dot{M}_{\text{Edd}}$ . In other words, any black hole source accreting above the Eddington limit is likely to have a scattering photosphere at several  $R_s$ . This fact is exploited by Mukai et al. (2003) and Fabbiano et al. (2003) in interpreting bright supersoft sources (including supersoft ULXs).

In PG1211+143 we estimate  $\dot{M} \sim 0.12 M_{\odot} \text{ yr}^{-1}$ . With  $\dot{M}_{\text{Edd}} = 0.4 M_{\odot} \text{ yr}^{-1}$ , appropriate for  $M = 4 \times 10^7 M_{\odot}$  (Kaspi et al. 2000), we find  $R_{\text{ph}} \simeq 100 R_s \sim 10^{15} \text{ cm}$ . This gives a blackbody temperature  $\sim 7 \times 10^4 \text{ K}$ , for a luminosity of  $4 \times 10^{45} \text{ erg s}^{-1}$ . This is lower than the fitted soft X-ray temperature; however, the emergent spectrum must be harder than the equivalent blackbody because of Comptonisation in the outflow. We also note that this material will be thermally unstable, perhaps providing an explanation of the lower ionisation matter required to fit some of the RGS absorption structure. We note, finally, that the physical size of the ‘X-ray photosphere’ is compatible with the observed soft X-ray variability.

### 4.3 The relativistic Fe K emission line

An important question raised by the existence of an optically thick photosphere above the inner disc is how the relativistic Fe K line could be seen. With the disc inside the launch radius of  $\sim 100 R_s$  (corresponding to an escape velocity of  $0.1c$ ) hidden from view, an extreme line would appear incompatible with the optically thick outflow, though a substantial area of the disc would remain visible in most geometries (and is probably required if the observed hard power law arises in a corona energised by magnetic reconnection). However, the detection of a large column density of highly ionised matter in the line-of sight to the hard X-ray source raises the possibility that the extreme ‘red wing’ evident between  $\sim 3\text{--}6 \text{ keV}$  in a simple power law fit to PG1211+143 is actually an artefact of absorption by more moderately ionised gas partially covering the X-ray source. Figure 10 shows such an alternative fit to the 1–10 keV EPIC spectrum of PG1211+143. This fit, with  $\Gamma \sim 2.04$ , retains the highly ionised outflow required to model the observed absorption lines, but now includes a second component, of column density  $2 \times 10^{23} \text{ cm}^{-2}$  and ionisation parameter  $\log \xi \sim 0.5$ , with a covering factor of  $\sim 0.42$ . The statistical quality of this fit is comparable to that including the LAOR line described in Section 3.2. The fit does still require an Fe K emission line, now described by a Gaussian profile with  $\sigma \sim 120 \text{ eV}$  and  $\text{EW} \sim 240 \text{ eV}$ , at an observed mean energy of  $\sim 6.0 \text{ keV}$  ( $\sim 6.5 \text{ keV}$  in the rest frame). We note this emission could arise by reflection from ionised matter in the disc beyond  $\sim 10 R_s$ , but could also include a significant component via re-emission from ionised gas in the outflow.

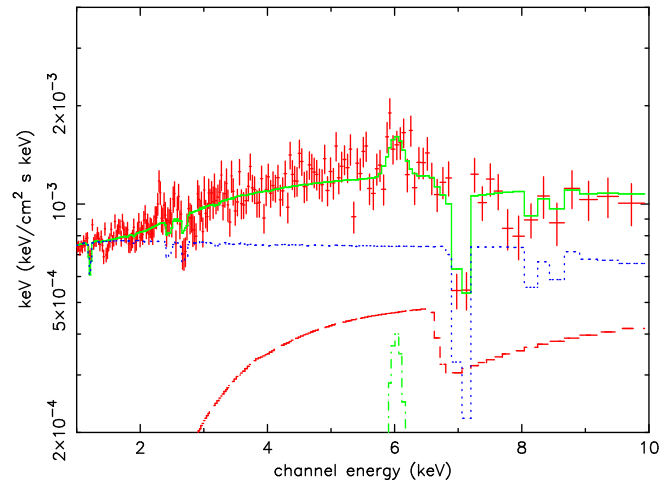


**Figure 10.** Unfolded spectrum of PG1211+143 modelled at 1–10 keV with a power law, Gaussian emission line and highly ionised outflow. The addition of a second, lower ionisation absorber covering  $\sim 0.45$  of the hard X-ray source replaces the relativistic broad Fe K of earlier fits.

### 4.4 The X-ray spectrum of PG1211+143, a high accretion rate AGN

The average 0.3–10 keV band luminosity of PG1211+143 during our *XMM-Newton* observation was  $\sim 10^{44} \text{ erg s}^{-1}$ . A simultaneous observation with the Optical Monitor on *XMM-Newton* (Mason et al. 2001) showed the energetically dominant BBB to be at a typical value, confirming the bolometric luminosity of order  $5 \times 10^{45} \text{ erg s}^{-1}$ . Together with the reverberation mass estimate for the SMBH in PG1211+143 of  $M \sim 4 \times 10^7 M_{\odot}$  (Kaspi et al. 2000) this luminosity implies accretion in PG1211+143 at close to the Eddington rate. We have argued previously that a high accretion rate may be the key to the characteristic X-ray properties of Narrow Line Seyfert 1 galaxies (eg Pounds and Vaughan 2000), and the present observation (of a Narrow Line Quasar) suggests a further signature of a high accretion rate may appear as Fe K absorption in a highly ionised and massive outflow.

### 4.5 Relation to Broad Absorption Line QSOs

Hitherto most evidence for extreme outflows has been found in UV studies of Broad Absorption Line (BAL) QSOs. The observation reported here, of a massive high velocity outflow from PG1211+143 broadens the scope of such studies. BAL QSOs show absorption in a variety of, mainly high-ionisation, UV resonance transitions with velocity widths up to  $\sim 30000 \text{ km s}^{-1}$  (e.g. Weymann et al. 1991). About 10% of optically selected QSOs display BALs. As BAL QSOs appear otherwise similar to non-BAL QSOs, an ‘orientation model’ is traditionally invoked in which BAL QSOs are those in which the particular line-of-sight intersects an outflow which may be intrinsic to all QSOs. This model has recently been questioned by the discovery of a relatively high fraction (15 – 20%) of radio-loud BAL quasars in the VLA FIRST survey bright quasar survey (Becker et al. 2000). Becker et al. propose BAL objects may be young or have recently been fueled. In any case, the higher fraction of quasars that have BALs implies a higher fraction of the line-of-sight to the

nucleus is covered with substantial absorbing material, consistent with the sort of covering factor we suggest above for PG1211+143.

Determining the amount of gas along the line-of-sight to a BAL is generally problematic due to a poor understanding of the relation between UV and X-ray absorption. The few BAL QSOs with useful X-ray spectra reveal complex absorption indicative of ionisation and/or partial covering (Gallagher et al. 2002). Fitting UV absorption lines suggests  $N_H \geq 10^{22} \text{ cm}^{-2}$ , whereas X-ray observations imply columns an order of magnitude or more higher (e.g. Hamann 1998; Sabra & Hamann 2001; Gallagher et al. 2002). Models in which the BAL gas is launched more or less vertically off a disk and then accelerated by radiation pressure (Murray et al. 1995; Murray & Chiang 1996; Elvis 2000) are reasonably consistent with the UV data but have difficulty in accelerating the large columns of material seen in X-rays unless they are launched from very close to the black hole (and hence are already moving at high velocity - as we propose for PG1211+143). In summary, while PG1211+143 has strong soft X-ray emission and is not a BAL QSO in the UV, it does display a large, fast moving outflow similar to that required to explain the BAL phenomenon. Whether the outflow in PG1211+143 becomes capable of producing BAL features further out in the flow but we simply do not intersect such a line of sight is unclear. Neither do we yet know how common such X-ray absorption features are in non-BAL QSOs. However, it seems likely that these phenomena are closely related.

## 5 CONCLUSIONS

(1) An *XMM-Newton* observation of the bright quasar PG1211+143 has revealed evidence of a massive high velocity outflow.

(2) One implication of the high column densities observed is that the inner flow will be optically thick, providing a natural explanation for the strong soft X-ray emission (and BBB) in PG1211+143.

(3) An extreme relativistic Fe K emission line apparent in a simple power law fit to the data can, alternatively, be explained in terms of partial covering of the continuum source by overlying matter in a lower ionisation state.

(4) We suggest the above properties might be common in AGN accreting at or close to the Eddington limit.

## ACKNOWLEDGEMENTS

The results reported here are based on observations obtained with *XMM-Newton*, an ESA science mission with instruments and contributions directly funded by ESA Member States and the USA (NASA). The authors wish to thank the SOC and SSC teams for organising the *XMM-Newton* observations and initial data reduction. ARK gratefully acknowledges a Royal Society Wolfson Research Merit Award.

## REFERENCES

Arnaud K.A. 1996, ASP Conf. Series, 101, 17

Bechtold J., Czerny B., Elvis M., Fabbiano G., Green R.F. 1987, ApJ, 314, 699

Becker, R.H., White, R.L., Gregg, M.D., Brotherton, M.S., Laurent-Muehleisen, S.A., Arav, N. 2000, ApJ, 538, 72

Chartas G., Brandt W.N., Gallagher S.C., Garmire G.P. 2002, ApJ, 569, 179

den Herder J.W. et al. 2001, A&A, 365, L7

Elvis M., Wilkes B., Giommi P., McDowell J. 1991, ApJ, 378, 537

Fabbiano, G., King, A.R., Zezas, A., Ponman, T.J., Rots, A., Schweizer, F. 2003, ApJ, in press

Fabian A.C., Iwasawa K., Reynolds C.S., Young A.J. 2000, PASP, 112, 1145

Fabian A.C. et al. 2002, MNRAS, 335, L1

Gallagher, S.C., Brandt, W.N., Chartas, G., Garmire, G.P. 2002, ApJ, 567, 37

Haardt F., Maraschi L. 1991, ApJ, 350, L81

Hamann, F. 1998, ApJ, 500, 798

Hasinger G., Schartel N., Komossa S. 2002, ApJ, 573, L77

Janiuk A., Czerny B., Madejski G.M. 2001, ApJ, 557, 408

Kallman T., Liedahl D., Osterheld A., Goldstein W., Kahn S. 1996, ApJ, 465, 994

Kaspi S. et al. 2000, ApJ, 533, 631

Kaspi S. et al. 2002, ApJ, 574, 643

Laor A. 1991, ApJ, 376, 90

Lee J.C., Reynolds C.S., Remillard R., Shultz N.S., Blackman E.G., Fabian A.C. 2002, ApJ, 567, 1102

Marziani P., Sulentic J.W., Dultzin-Hacyan D., Clavani M., Moles M. 1996, ApJS, 104, 37

Mukai, K., Pence, W.D., Snowden, S.L., Kuntz, K.D. 2003, ApJ, in press (astro-ph/0209166)

Murphy E.M., Lockman F.J., Laor A., Elvis M. 1996, ApJS, 105, 369

Nandra K., George I.M., Mushotzky R.F., Turner T.J., Yaqoob T. 1997, ApJ, 477, 602

Palmeri P., Mendoza C., Kallman T.R., Bautista M.A. 2002, ApJ, 577, L119

Pounds K.A., Nandra K., Stewart G.C., George I.M., Fabian A.C. 1990, Nature, 344, 132

Pounds K.A., Vaughan S. 2000, New Astron. Rev., 44, 431

Pounds K.A., Reeves J.N., O'Brien P.T., Page K.A., Turner M.J.L., Nayakshin S. 2001, ApJ, 559, 181

Pounds K.A., Reeves J.N. 2002, in: *New Visions of the X-ray Universe in the XMM-Newton and Chandra era* ed. F. Jansen, (astro-ph/0201436)

Pounds K.A., Reeves J.N., Page K.L., Wynn G.A., O'Brien P.T. 2003, MNRAS, in press

Reeves J.N., Turner M.J.L., Ohashi T., Kii T. 1997, MNRAS, 292, 468

Reeves J.N., Wynn G., O'Brien P.T., Pounds K.A. 2002, MNRAS, 336, L56

Reynolds C.S., Nowak M.A. 2002, astro-ph/0212065

Sabra, B.M., Hamann, F. 2001, ApJ, 563, 555

Sabra, B.M., Hamann, F., Jannuzi, B.T., George, I.M., Shields, J.C. 2003, ApJ, 2003, in press (astro-ph/0302555).

Sako M. et al. 2001, A&A, 365, L168

Saxton R.D., Turner M.J.L., Williams O.R., Stewart G.C., Ohashi T., Kii T. 1993, MNRAS, 262, 63

Strüder L. et al. 2001, A&A, 365, L18

Turner M.J.L. et al. 2001, A&A, 365, L27

Weymann, R.J., Morris, S.L., Foltz, C.B., Hewitt, P.C. 1991, ApJ, 373, 23

Yaqoob T., Serlemitsos P., Mushotzky R., Madejski G., Turner T.J., Kunieda H. 1994, PASJ, 46, L173